BULLETIN OF THE POLISH ACADEMY OF SCIENCES
TECHNICAL SCIENCES, Vol. 68, No. 3, 2020
DOI: 10.24425/bpasts.2020.133369

Sensorless five-phase induction motor drive with third harmonic injection and inverter output filter

P. STRANKOWSKI, J. GUZINSKI*, M. MORAWIEC, A. LEWICKI, and F. WILCZYNSKI

Gdansk University of Technology, Electrical and Control Engineering Faculty, 11/12 Gabriela Narutowicza Street, 80-233 Gdańsk, Poland

Abstract. The paper presents a sensorless control approach for a five-phase induction motor drive with third harmonic injection and inverter output filter. In the case of the third harmonic injection being utilised in the control, the physical machine has to be divided into two virtual machines that are controlled separately and independently. The control system structure is presented in conjunction with speed and rotor flux observers that are required for a speed sensorless implementation of the drive. The last section is dedicated to experimental results of the drive system in sensorless operation, and the uninterrupted drive operation for two open-phase faults.

Key words: sensorless control, five-phase induction motor, inverter output filter, multiscalar control.

1. Introduction

The development of three-phase machines is in continuous progress. New sophisticated control methods were invented in conjunction with higher fault-tolerant algorithms, to ensure higher efficiency, as well as higher reliability [1]. Nevertheless, the progress in the power electronics area and accompanying decreasing prices for semi-conductors are making multiphase with a phase number higher than three, increasingly attractive.

The five-phase induction motor is the most prominent representative in this field. The possibility of torque enhancement through the third harmonic injection in combination with high robustness make this machine significant competition to the three-phase induction motor [2–5]. Moreover, this drive system excels with its fault tolerance when one or even two non-adjacent phases are opened. This could be especially important in applications that require high responsibility. Nevertheless, due to the higher number of phases, the voltage generation requires a more complicated vector modulation [6–8], and when the third harmonic is injected, the control system is more complex [1–5, 9, 10].

A further component that improves the reliability of a drive system is the inverter output filter, or LC filter [10–12]. The application of this kind of filter is especially important for drive systems with long supply cables, e.g. elevators, cranes and earth deep hole pumping stations. Additional LC components act as low-pass filters in each phase that change the rectangular-shape waveform of the inverter output voltage to a nearly smooth sinusoidal shape. The benefits of the reduced voltage raise dv/dt are for instance less stressed stator insulation, and reduction of the harmful common mode current that is especially important for motor bearings. All these improvements lead to overall life-time increase of the motor. However, the LC filter makes the operation of the drive control system complex, especially in speed sensorless drives. This is explained through differences between inverter output and motor input voltages and current. The differences in voltages could be up usually to 4.5% in magnitude and few degrees in phase-shift. In other words, the LC filter is an element outside the inverter, but the control algorithm is in general based on the inverter internal voltage and current sensors. The solutions to these problems are presented in [10, 13, 14], which are mainly based on the LC filter model introduction into estimation and control. In this regard the proper and applicable method for multiphase drives is still unique and only proposed in [15–17], in which the multiscalar control structure has been used [18]. It is worth mentioning, that the less popular multiscalar control is one of the drive control methods that is mostly known to be used for sensorless speed control and is partially similar to methods that are known as nonlinear control [19]. The multiscalar control has been recently implemented for multiphase drives without LC filter in [9, 20] and with LC filter in [15–17].

This paper focuses on the five-phase drive, whose general structure has been presented in Fig. 1.

To illustrate an advanced multiphase drive configuration, the paper includes sensorless control that utilizes the 3rd harmonic injection in conjunction with the inverter output filter. In contrast to [15] and [16], a simplified control structure is presented, in which the LC filter is taken into account in the control process, but the number of controllers is kept identical as used for a conventional drive without a LC filter, as mentioned in [17].

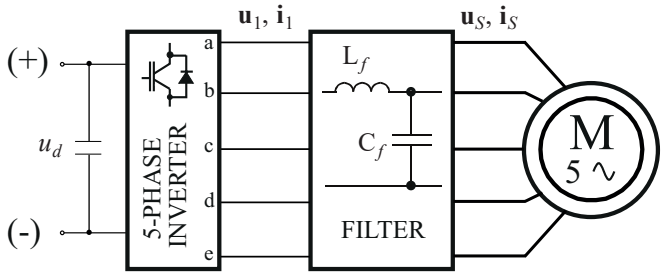

Fig.1. Structure of the five-phase induction motor drive with LC filter

*e-mail: jaroslaw.guzinski@pg.edu.pl

Manuscript submitted 2019-11-29, revised 2020-01-27, initially accepted for publication 2020-02-13, published in June 2020

The control is based on two multiscalar control systems, which allow an independent control of the 1st and 3rd harmonic rotor flux components. To meet the requirements of sensorless control, two observers were implemented that estimated the rotor angular speed and rotor flux. In all these structures, the presence of the inverter output filter is considered.

The last section of the presented paper is dedicated to the experimental results that demonstrate the function of the drive, and the extraordinary operation with one or two non-adjacent open phases. These experimental results for healthy and faulty drive operation confirm the correct and robust operation of the drive.

2. Control System

The torque improvement in five-phase drives is possible, by injecting the third harmonic, up to 15% as reported in [21] and [22]. The utilization of third harmonic voltages and currents leads to quasi-trapezoidal flux distribution [1–5, 7, 20]. To achieve the highest performance, a machine with concentrated windings is indispensable, which practically means one stator slot per pole and coil. The separation of the machine's natural variables into two independent virtual machines is possible with the transformation matrix in Eq. (1):

$$\begin{bmatrix} i_{\alpha 1} \\ i_{\beta 1} \\ i_{\alpha 3} \\ i_{\beta 3} \\ i_o \end{bmatrix} = \sqrt{\frac{2}{5}} \begin{bmatrix} 1 & \cos\left(\frac{2\pi}{5}\right) & \cos\left(\frac{4\pi}{5}\right) & \cos\left(\frac{4\pi}{5}\right) & \cos\left(\frac{2\pi}{5}\right) \\ 0 & \sin\left(\frac{2\pi}{5}\right) & \sin\left(\frac{4\pi}{5}\right) & -\sin\left(\frac{4\pi}{5}\right) & -\sin\left(\frac{2\pi}{5}\right) \\ 1 & \cos\left(\frac{4\pi}{5}\right) & \cos\left(\frac{8\pi}{5}\right) & \cos\left(\frac{8\pi}{5}\right) & \cos\left(\frac{4\pi}{5}\right) \\ 0 & \sin\left(\frac{4\pi}{5}\right) & \sin\left(\frac{8\pi}{5}\right) & -\sin\left(\frac{8\pi}{5}\right) & -\sin\left(\frac{4\pi}{5}\right) \\ \frac{1}{\sqrt{2}} & \frac{1}{\sqrt{2}} & \frac{1}{\sqrt{2}} & \frac{1}{\sqrt{2}} & \frac{1}{\sqrt{2}} \end{bmatrix} \cdot \begin{bmatrix} i_a \\ i_b \\ i_c \\ i_d \\ i_e \end{bmatrix} \quad (1)$$

This matrix allows a separation of the physical machine into two virtual machines – 1st and 3rd harmonic, or 1st and 2nd coordinate systems, respectively (Fig. 2).

The implementation of a drive with 3rd harmonic injection thereby requires two independent voltage modulation procedures, control systems and a synchronization unit.

A control system that proved reliable operation in this configuration is the control based on mutliscalar variables, as presented in [9, 10, 16, 19, 20, 23].

The multiscalar control variables are denoted as follows [9]:

$$x_{11}^{(I)} = \omega_r^{(I)} \quad (2)$$

$$x_{12}^{(i)} = \psi_{r\alpha}^{(i)} i_{s\beta}^{(i)} - \psi_{r\beta}^{(i)} i_{s\alpha}^{(i)} \quad (3)$$

$$x_{21}^{(i)} = \psi_{r\alpha}^{2(i)} + \psi_{r\beta}^{2(i)} \quad (4)$$

$$x_{22}^{(i)} = \psi_{r\alpha}^{(i)} i_{s\alpha}^{(i)} + \psi_{r\beta}^{(i)} i_{s\beta}^{(i)} \quad (5)$$

where x_{11} is the rotor angular speed, x_{12} is proportional to the torque, x_{21} is the square of the rotor flux vector products, and x_{22} is the scalar product of the stator current vector and rotor flux vector. The superscript (i) describes the applied orthogonal plane for the 1st and 3rd harmonic (noted as I and II respectively).

The control system structure is illustrated in Fig. 3.

The complete control system includes two independent sub-control systems for the 1st harmonic and for the 3rd harmonic, respectively. This allows independent control of the rotor flux, which is required to generate a quasi-trapezoidal rotor flux distribution. The only difference between the 1st and 2nd control system is that the speed controller in the 1st plane is replaced with a rotor flux speed controller, whose input is provided by the synchronisation unit, as presented in [9, 15, 17, 20]. After the decoupling of the non-linear system and the LC filter consideration, the desired voltages are delivered to the five-phase Pulse Width Modulation (PWM) routine,

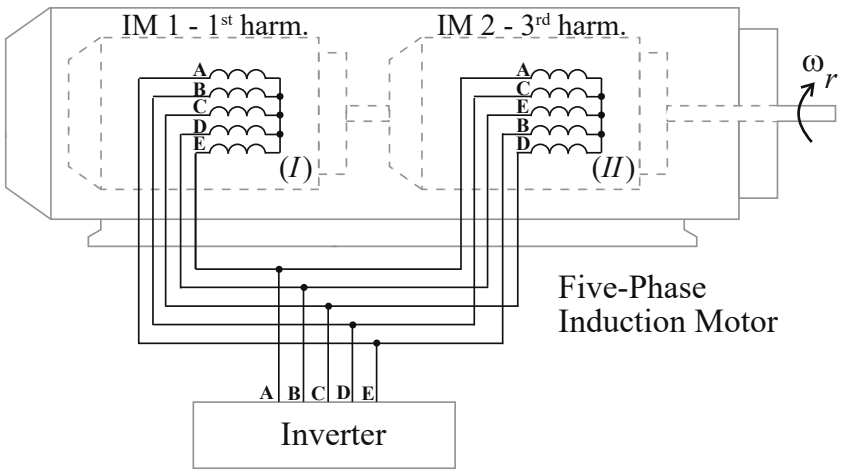

Fig. 2. Schematic representation of the concept of five-phase induction motor control with 3rd harmonic injection

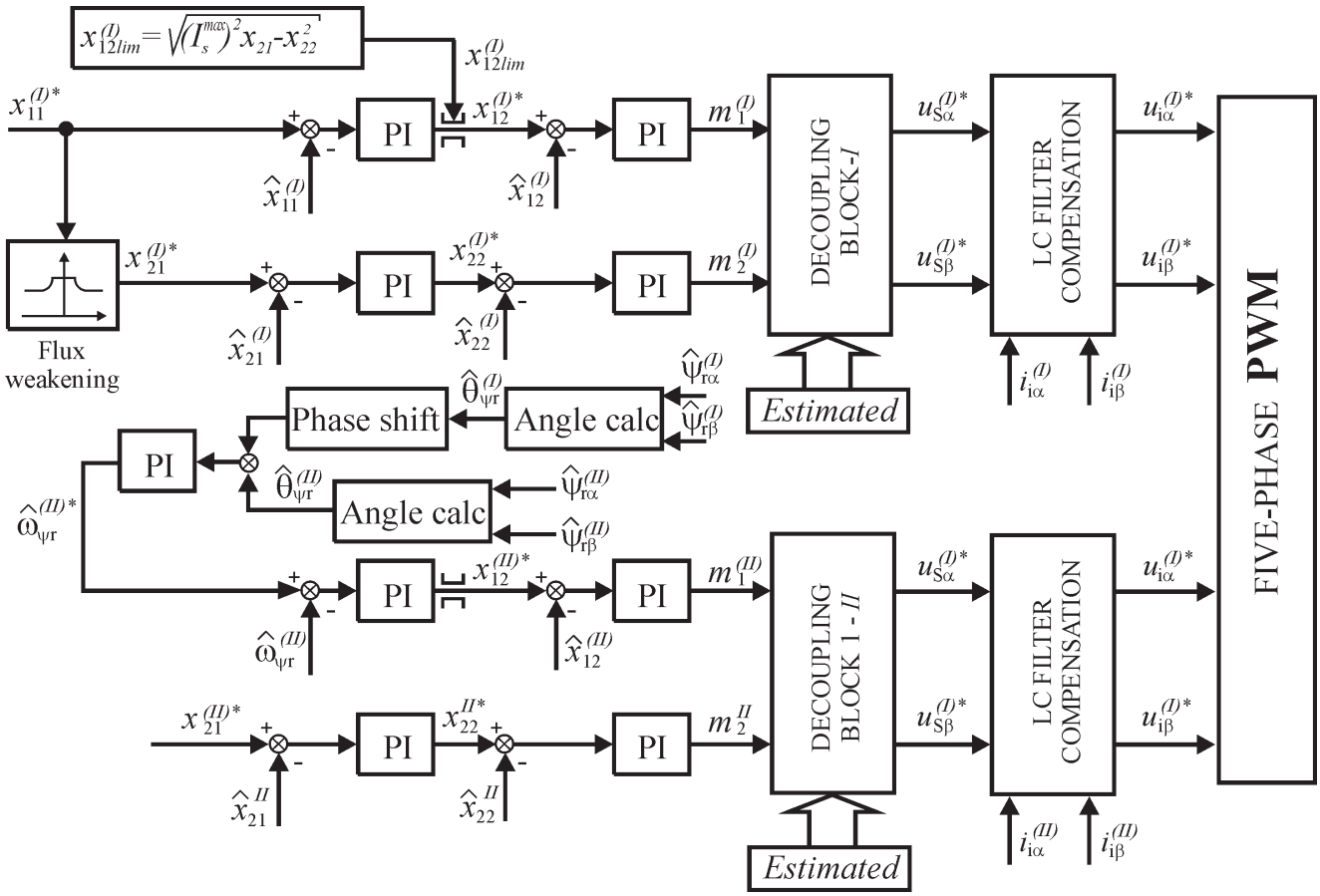

Fig. 3. Multiscalar control structure with 3rd harmonic injection and rotor flux synchronisation

which generates two, independent voltages for each virtual machine [8].

The inverter output filter is located in the control system to ensure reliable drive operation. Several propositions have been presented. However, the solution to overcome this problem, which is proposed in [10, 13, 14, 24] requires an additional subordinate control system, with coordinates transformation and further two or four PI controllers for the three-phase induction motor. That means that the application of this solution in two control planes, which is the case of the five-phase induction motor drive, will require consideration of four or eight additional PI controllers [15, 16]. The concept presented there offered good control properties, but requires PI controller tuning. This increases the level of complexity and involves much more computing time, which is very limited in the microprocessor for a multiphase drive.

Furthermore, to be able to accomplish the main tasks for the control, a compromise solution has to be found, which would reduce the computational effort of the LC filter control. The proposed solution is based on filter inductance voltage drop calculations, as denoted in (6).

$$\hat{u}_{1\alpha}^{(i)} = L_f \frac{di_{1\alpha}^{(i)}}{d\tau}, \qquad \hat{u}_{1\beta}^{(i)} = L_f \frac{di_{1\beta}^{(i)}}{d\tau} \tag{6}$$

The filter current differentials of $i_{1\alpha}$ and $i_{1\beta}$, calculated each time in the observer, presented in the next section, are used to calculate the magnitude of the resulting voltage drop on the filter inductance:

$$\left|U_1^{(i)}\right| = L_f \sqrt{\left(\frac{di_{1\alpha}^{(i)}}{d\tau}\right)^2 - \left(\frac{di_{1\beta}^{(i)}}{d\tau}\right)^2} \tag{7}$$

where $|U_1|$ is the output filter inductance voltage drop.

However, it is known that the differentials are sensitive to fast changes, which are likely to occur in the PWM supply drive. To limit these unwanted effects, the filtration was used:

$$\left|U_{1F}^{(i)}\right| = \left(L_f \sqrt{\left(\frac{di_{1\alpha}^{(i)}}{d\tau}\right)^2 - \left(\frac{di_{1\beta}^{(i)}}{d\tau}\right)^2} - \left|U_{1F}^{(i)}\right| \right) k_f \tag{8}$$

where $|U_{1F}|$ is a temporary variable for filtering the differentials, and k_f d is the filter coefficient.

The filtered voltage drop is added to the desired voltage of the control system before the execution of the PWM routine. This voltage drop compensation serves as support of the control system in both planes (Fig. 4).

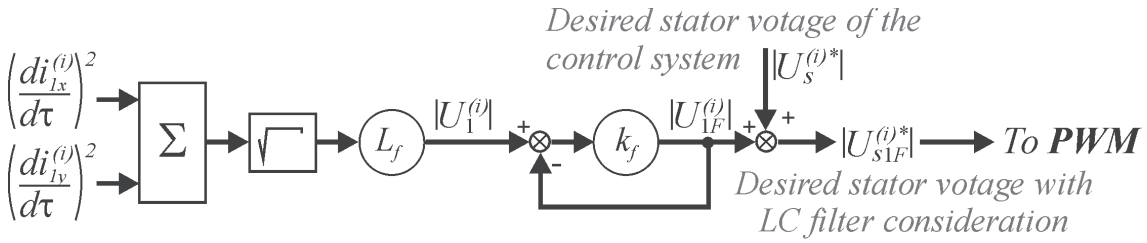

Fig. 4. LC filter inductance voltage drop compensation used in control system

A situation with no voltage drop consideration that leads to oscillations in the drive system, especially in the higher speed range when the voltage drop caused by the filter inductance is higher.

The used voltage drop consideration is not the most optimal solution, compared to the solutions mentioned e.g. in [10, 13, 14, 24], mainly due to the fact that the concern of the phase shift between inverter output and motor input is not addressed. However, the experimental investigations have shown that in this particular case the voltage drop consideration helped the drive system overcome the main difficulty related to the presence of the filter with very low computational effort, which was the compromise that had to be made in the experiment, and was an essential prerequisite for putting the drive into operation.

3. Sensorless control

For the sensorless control, the selection of the appropriate speed observer is indispensable. Furthermore, if the 3rd harmonic is injected, a second observer is required for the virtual machine. In case that an inverter output filter is installed to the drive system this structure has to be included in the estimation procedure.

The speed observer that is used in the control system is an enhanced version of the speed observer structure introduced by Krzemiński for three-phase machines [25], and includes the capacitor voltage calculation with simultaneous filtration of the calculation.

The complete speed observer equations are denoted as follows [17]:

$$\frac{d\hat{\mathbf{i}}_s^{(I)}}{d\tau} = a_1^{(I)}\cdot\hat{\mathbf{i}}_s^{(I)} + a_2^{(I)}\cdot\hat{\boldsymbol{\psi}}_r^{(I)} - ja_3\cdot\hat{\boldsymbol{\zeta}}^{(I)} + \\ + a_4^{(I)}\cdot\left(\hat{\mathbf{u}}_c^{(I)} + \left(\hat{\mathbf{i}}_1^{(I)} - \hat{\mathbf{i}}_s^{(I)}\right)\cdot R_f\right) + \\ + k_1^{(I)}\cdot\left(\hat{\mathbf{i}}_1^{(I)} - \mathbf{i}_1^{(I)}\right) \tag{9}$$

$$\frac{d\hat{\boldsymbol{\psi}}_r^{(I)}}{d\tau} = a_5^{(I)}\cdot\hat{\boldsymbol{\psi}}_r^{(I)} + a_6^{(I)}\cdot\hat{\mathbf{i}}_s^{(I)} + j\hat{\boldsymbol{\zeta}}^{(I)} + \\ + jk_2^{(I)}\cdot\left(\hat{\boldsymbol{\zeta}}^{(I)} - \hat{\omega}_r\cdot\hat{\boldsymbol{\psi}}_r^{(I)}\right) \tag{10}$$

$$\frac{d\hat{\boldsymbol{\zeta}}^{(I)}}{d\tau} = a_5^{(I)}\cdot\hat{\boldsymbol{\zeta}}^{(I)} + j\hat{\omega}_r\cdot\hat{\boldsymbol{\zeta}}^{(I)} + a_6^{(I)}\cdot\hat{\mathbf{i}}_s^{(I)}\cdot\hat{\omega}_r + \\ + k_3^{(I)}\cdot\left(\hat{\mathbf{i}}_1^{(I)} - \mathbf{i}_1^{(I)}\right) \tag{11}$$

$$\frac{d\hat{\mathbf{u}}_c^{(I)}}{d\tau} = \left(\frac{\left(\hat{\mathbf{i}}_1^{(I)} - \hat{\mathbf{i}}_s^{(I)}\right)}{C_f} - \hat{\mathbf{u}}_c^{(I)}\right)\cdot k_4^{(I)} \tag{12}$$

$$\frac{d\hat{\mathbf{i}}_1^{(I)}}{d\tau} = \frac{\mathbf{u}_s^{*(I)} - R_{ind}\cdot\hat{\mathbf{i}}_1^{(I)} - R_f\cdot\left(\hat{\mathbf{i}}_1^{(I)} - \hat{\mathbf{i}}_s^{(I)}\right) - \hat{\mathbf{u}}_c^{(I)}}{L_f} + \\ + k_5^{(I)}\cdot\left(\hat{\mathbf{i}}_1^{(I)} - \mathbf{i}_1^{(I)}\right) + jk_6^{(I)}\cdot\left(\hat{\mathbf{i}}_1^{(I)} - \mathbf{i}_1^{(I)}\right) \tag{13}$$

$$\hat{\omega}_r = \frac{\hat{\zeta}_\alpha^{(I)}\hat{\psi}_{r\alpha}^{(I)} + \hat{\zeta}_\beta^{(I)}\hat{\psi}_{r\beta}^{(I)}}{\hat{\psi}_{r\alpha}^{2(I)} + \hat{\psi}_{r\beta}^{2(I)}} \tag{14}$$

where the hat operator ^ indicates estimated values of next vectors: $\mathbf{i}_s$ stator current, $\boldsymbol{\psi}_r$ rotor flux, $\boldsymbol{\zeta}$ electromotive force, $\mathbf{u}_c$ capacitor voltage, $\mathbf{i}_1$ inverter output current. Moreover, $k_1 \ldots k_6$ are the observer gains, R_f the filter damping resistance and $\mathbf{u}_s^*$ is the stator reference voltage. The coefficients $a_1 \ldots a_6$ are defined in relation to motor parameters as follows:

$$a_1 = -\left(R_s L_r^2 + R_r L_m^2\right)/L_r w_\sigma, \\ a_2 = R_r L_m/L_r w_\sigma,\ a_3 = L_m/w_\sigma,\ a_4 = L_r/w_\sigma, \\ a_5 = R_r L_m/L_r,\ a_6 = -R_r/L_r,\ w_\sigma = L_r L_s - L_m^2 \tag{15}$$

where L_s, L_r and L_m are the stator, rotor and mutual inductances, R_r and R_s are the resistances for rotor and stator and have to be calculated separately for the 1st and 2nd plane, because the five-phase induction motor parameters are different in each plane (Table 1).

The machine parameters were determined with conventional idle and short circuit tests. However, the two tests were performed by supplying only the 1st harmonic and subsequently the 2nd plane completely independent from each other.

The most important state variable for the 2nd plane control system is the rotor flux. For this reason, a rotor flux observer is only needed. The more compact observer is also beneficial in terms of computational effort in the control structure. In the

Table 1
Parameters of a five-phase induction motor

Parameter	Value
Power	5.5 kW
Current	8.8 A
Voltage (phase)	173 V
Frequency	50 Hz
No load speed	1500 rpm
Parameters for the 1st plane	
Stator resistance	1.04 Ω
Rotor resistance	1.69 Ω
Stator, rotor leakage inductance	11 mH
Mutual inductance	286 mH
Parameters for the 2nd plane	
Stator resistance	1.04 Ω
Rotor resistance	2.56 Ω
Stator, rotor leakage inductance	9 mH
Mutual inductance	48 mH

presented control system, most of the available calculation time is used by the PWM and the control system. For this reason, the selected observer for the 3rd harmonic injection has to be as small as possible but as precise as possible to ensure a rotor flux estimation in nominal conditions, which is in the 3rd harmonic at 150 Hz. The rotor flux observer that is used for the 2nd plane is a modified version of the Luenberger observer presented in [23], and is denoted in (15–19):

$$\frac{d\hat{\mathbf{i}}_s^{(II)}}{d\tau} = a_1^{(II)} \cdot \hat{\mathbf{i}}_s^{(II)} + a_2^{(II)} \cdot \hat{\boldsymbol{\psi}}_r^{(II)} + ja_3^{(II)} \cdot \hat{\boldsymbol{\psi}}_r^{(II)} \cdot \hat{\omega}_r^{II} + \\ + a_4^{(II)} \cdot \left(\hat{\mathbf{u}}_c^{(II)} + \left(\hat{\mathbf{i}}_1^{(II)} - \hat{\mathbf{i}}_s^{(II)} \right) \cdot R_f \right) + \\ + k_1^{(II)} \cdot \left(\hat{\mathbf{i}}_1^{(II)} - \mathbf{i}_1^{(II)} \right) \tag{16}$$

$$\frac{d\hat{\boldsymbol{\psi}}_r^{(II)}}{d\tau} = a_5^{(II)} \cdot \hat{\boldsymbol{\psi}}_r^{(II)} + a_6^{(II)} \cdot \hat{\mathbf{i}}_s^{(II)} + j\hat{\omega}_r^{II} \cdot \hat{\boldsymbol{\psi}}_r^{(II)} + \\ = k_2^{(II)} \cdot \left(\hat{\mathbf{i}}_1^{(II)} - \mathbf{i}_1^{(II)} \right) - k_3^{(II)} \cdot \hat{\omega}_r^{II} \cdot \left(\hat{\mathbf{i}}_1^{(II)} - \mathbf{i}_1^{(II)} \right) \tag{17}$$

$$\frac{d\hat{\mathbf{u}}_c^{(II)}}{d\tau} = \left(\frac{\left(\hat{\mathbf{i}}_1^{(II)} - \hat{\mathbf{i}}_s^{(II)} \right)}{C_f} - \hat{\mathbf{u}}_c^{(II)} \right) \cdot k_4^{(II)} \tag{18}$$

$$\frac{d\hat{\mathbf{i}}_1^{(II)}}{d\tau} = \frac{\mathbf{u}_{s\alpha}^{*(II)} - R_{ind} \cdot \hat{\mathbf{i}}_1^{(II)} - R_f \cdot \left(\hat{\mathbf{i}}_1^{(II)} - \hat{\mathbf{i}}_s^{(II)} \right) - \hat{\mathbf{u}}_c^{(II)}}{L_f} + \\ + k_5^{(II)} \cdot \left(\hat{\mathbf{i}}_1^{(II)} - \mathbf{i}_1^{(II)} \right) \tag{19}$$

$$\hat{\omega}_r^{II} = -3\hat{\omega}_r^{I} \tag{20}$$

According to the speed observer in the 1st plane, the capacitor voltage is calculated with simultaneous filtration of the variable. The rotor speed that is required for the flux estimation is calculated based on the rotor speed estimation Eq. (20).

4. Experimental results

The experimental results are dedicated to the sensorless operation, and to the open phase fault-tolerant operation for which the five-phase induction motor stands out. The drive system consists of a voltage inverter (nominal power 5.5 kW, FPGA – Altera Cyclon II, DSP – ADSP-21363), a five-phase induction motor (Table 1), and an inverter output filter ($L_f = 5$ mH, $C_f = 14$ μF, $R_f = 1.1$ Ω). In order to meet the requirements of sensorless operation, only the inverter output currents and the DC-link voltage are measured. Based on these variables, the rotor speed is calculated. All observer gains were initially determined in the simulation research, and tuned in the experimental test setup.

The first result (Fig. 5) illustrates the resulting rotor flux distribution, the vector component of the estimated rotor flux in the 1st and 2nd control plane, and the synchronisation error in steady state conditions at a rotor speed of 0.3 p.u.

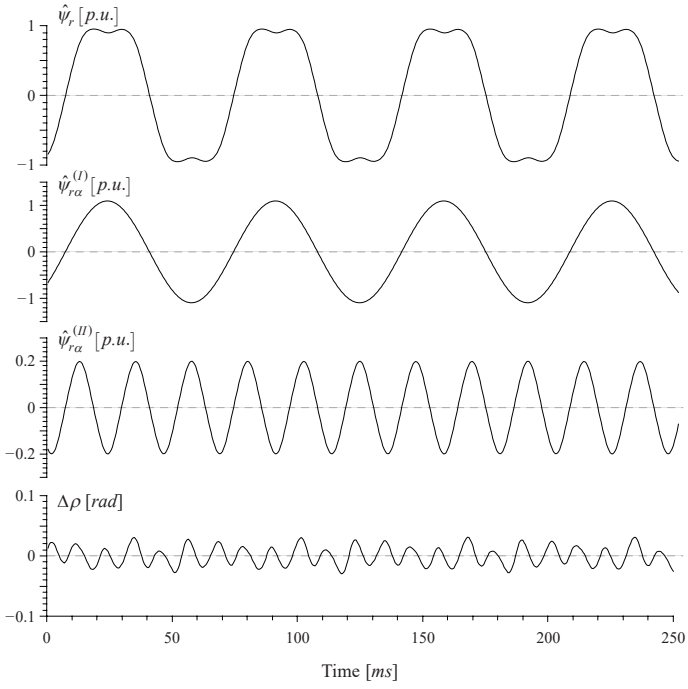

Fig. 5. Rotor flux vector components – resulting rotor flux, rotor flux vector component in 1st and 2nd plane, and synchronisation error

As can be seen in Fig. 5, the resulting rotor flux distribution is quasi-rectangular with a peak value of 1.0 p.u. In order to reach this peak value, the vector component of the rotor flux estimation has to reach a value of 1.2 p.u., and the amplitude of the 2nd control system has to provide a value of 0.2 p.u. During the complete sequence, the highest amplitude of the synchro-

nisation error is less than 0.05 rad. A low error is especially mandatory here for a continuous and stable synchronisation of both rotor flux components.

The next experiment (Fig. 6 and Fig. 7) demonstrates the multiscalar variables of both control systems.

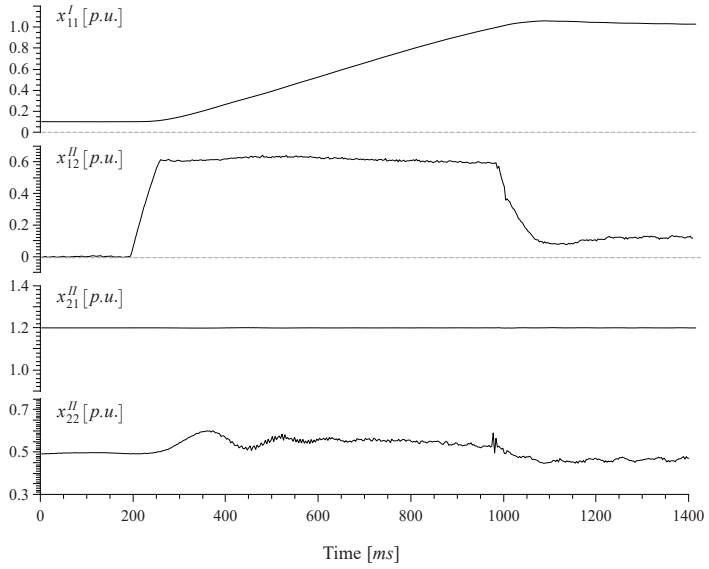

Fig. 6. Multiscalar variables in 1st plane

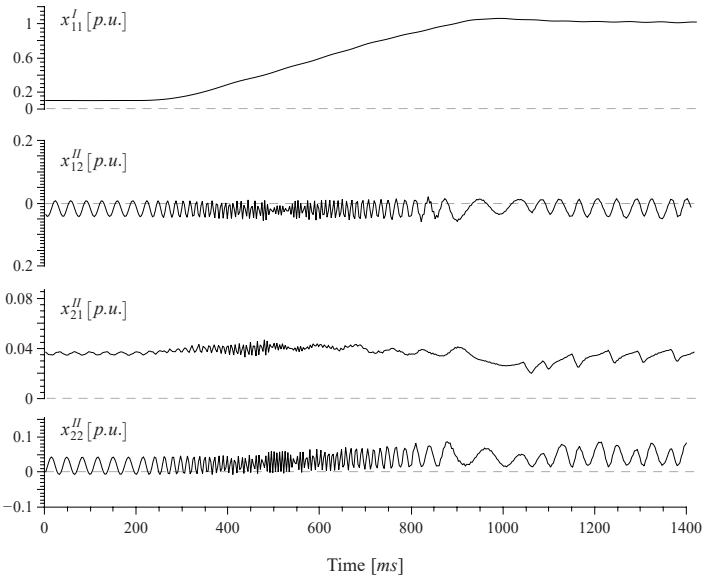

Fig. 7. Multiscalar variables in 2nd plane

The multiscalar variables for the 1st control plane are presented in Fig. 6 during a motor speed change from 0.2 p.u. to 1.0 p.u., and as expected, the speed change causes an increase of the x_{12} variable, which represents the torque of the 1st plane machine. The x_{21} variable, which mirrors the rotor flux of the machine, presents a stable and continuous transient during the complete record. However, the control variable x_{22} presents oscillations, which do not interfere with the drive operation as can be seen in the rotor speed which is represented by the x_{11} variable.

Figure 7 demonstrates the multiscalar variables in the 2nd control plane for an identical speed change, as presented in Fig. 6. In contrast to the multiscalar variables in the 1st plane, the 2nd plane multiscalar variables are oscillating. The torque variable is also different and negative. The negative torque component is required here to obtain a positive torque on the driving shaft (Eq. (20)). The flux component x_{21} also shows oscillations. However, it holds a mean value of 0.035 p.u., which is mandatory to achieve a quasi-rectangular rotor flux distribution.

It has to be underlined here, that the 2nd plane control system operates at frequency three times higher, which, in nominal conditions, is 150 Hz. This high frequency makes the estimation of the rotor flux in conjunction with the low current and voltage values an exceptionally complex task.

The next experiment (Fig. 8) presents a speed reversal of the machine from 0.02 p.u. to – 0.02 p.u., where the resulting rotor flux distribution, the estimated and measured speed and the synchronisation error is presented.

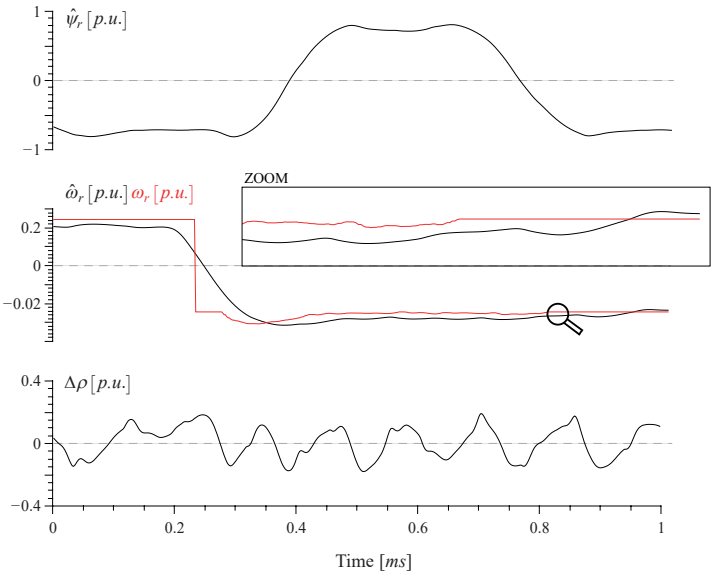

Fig. 8. Low speed reversal – resulting rotor flux component, measured and estimated rotor speed, and synchronization error

As showed in Fig. 8, the operation at lower speed is possible with the 3rd harmonic injection and the resulting rotor flux distribution is maintained during the complete sequence. This operation point is extraordinary difficult for the reason that the 3rd harmonic was here injected and synchronized with the fundamental. Everything was performed in a sensorless operation in conjunction with the inverter output filter. The error of the estimated rotor speed is approx. 0.5% – considering the full range of speed estimation. Nevertheless, minor oscillations could be also caused by interactions in the control system. The synchronisation error oscillates with a peak value of 0.2 p.u.

5. Open-phase fault operation possibility

The most promising advantage of a five-phase induction motor drive is the ability to provide torque with one or two non-adjacent phases [2–3, 26–30]. This advantage is paid with a current increase of the remaining healthy phases. However, this current increase is in contrast to three-phase machines, at an uncritical level.

The following experiments present the open-phase operation possibility of the drive system to prove the uninterrupted operation of the proposed sensorless control. It has to be mentioned here that no post-fault countermeasures, e.g. control parameters or voltage modulation, were taken during the experiments. Moreover, the 3rd harmonic injection was deactivated for this test for the reason that the synchronisation was lost during this experiment, and the attempts of the synchronisation control unit to synchronise the 2nd control system would only disturb the drive operation.

Figure 9 presents the transients of the measured inverter output currents in each phase.

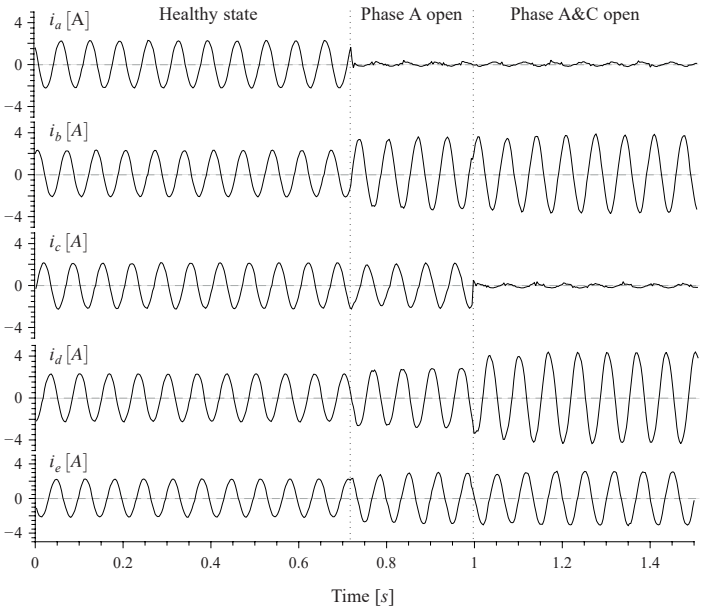

Fig. 9. Phase currents transients during successive deactivation of phases A and C

The first phase deactivation (Fig. 9) causes an increase in the remaining phases. However, continuous and uncritical operation of the drive is still possible. Next, the deactivation of phase C causes a further current increase in the remaining three phases, but at an uncritical level for the machine. A minimal current flow is still recognisable for the reason that the inverter output filter is installed.

The change of this phase symmetry is also clearly visible in an xy-diagram of the inverter output current vector component (Fig. 10).

The trajectory of the inverter output current vector is circular in healthy conditions and changes to elliptical if phase A is

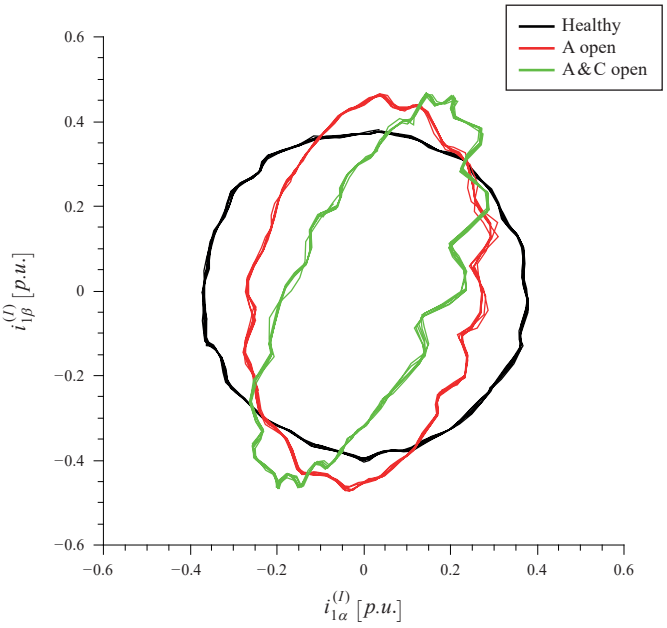

Fig. 10. Measured inverter output current vector components – healthy state (black), phase A open (red), and phases A and C open (green)

deactivated. If phases A and C are deactivated, the elliptical change is then intensified, which indicates also the lag of symmetry in the five-phase system.

To emphasise the open phase operation possibility, the following experiment (Fig. 11) presents the rotor direction change from negative nominal rotor speed to nominal speed. It has to be mentioned here that the control system worked even in this faulty condition in the sensorless configuration, which underlines the stable operation of the observer in this critical state.

Figure 11 illustrates the measured rotor speed and the estimated rotor speed with phase A open (black), and with phases A and C open (red). Even the critical zero frequency transition did not cause any interference, which could be seen as extraordinary for the speed observer that was applied here. The

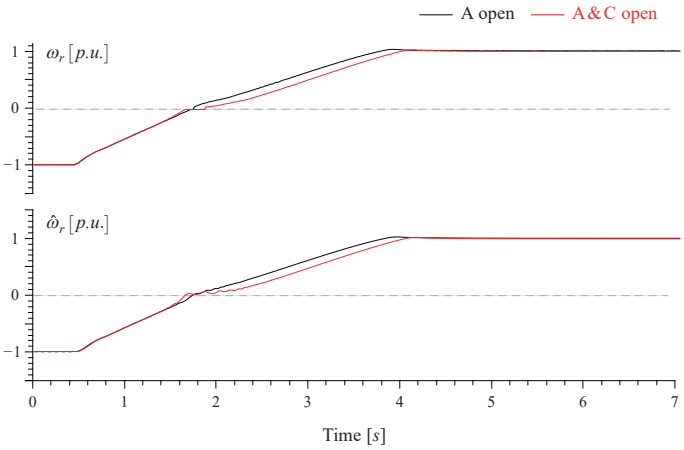

Fig. 11. Measured and estimated rotor speed during motor reversal with phase A, and phase A and C opened

direction change with two opened phases is slower, which is mainly caused due to the current limitation of the control system to ensure safe operation of the drive. However, such an operation is possible even with two opened phases, which can be considered outstanding.

6. Conclusion

The paper presented the sensorless operation of a five-phase induction motor drive with inverter output filter and 3rd harmonic injection. The multiscalar control system structure was presented, which included two independent control systems and a synchronisation unit. Such a structure was required to allow independent control of both virtual machines and to archive the quasi-trapezoidal resulting rotor flux distribution. To meet the requirements of speed sensorless control two observers have been presented for the speed estimation in the 1st plane system, and rotor flux estimation in the 2nd plane. The presented observers ensured stable properties in nominal condition, which is 150 Hz for the 2nd plane. Even in low speed operation the system was stable with synchronisation of the 3rd harmonic and proved to be a difficult operation point. However, the major advantage of the proposed observer is its stability to parameter changes of the machine, which was proved with the demonstration of the open-phase uninterrupted operation capability. It should be underlined here that the novelty was in the observer structures in which a simultaneous calculation and filtration of the capacitor voltage drop value was performed that enabled the quality of this operation.

The last section was dedicated to the verification of the drive operation with one or two non-adjacent phases. It has to be mentioned here, that no control parameters have been changed during this experiment. The fault tolerance of the presented control system also allowed a direction reversal with two opened phases in the sensorless configuration. This extraordinary fault tolerance underlines the high responsibility of the proposed sensorless drive, which is outstanding compared to three-phase drives. Furthermore, the injection of the third harmonic enables a higher material exposure of the stator that is gained through the introduction of a second control system with rotor flux synchronization. This is especially important for the industry, for the reason that this additional torque generation could be implemented without the need to increase the production costs of the machine.

Acknowledgements This work was supported by the National Science Centre of Poland grant no. 2015/19/N/ST7/03078

References

[1] Z. Liu, Y. Li, and Z. Zheng, "A Review of drive techniques for multiphase machines", *CES Trans. on Electrical Machines and Systems* 2(2), 243–351 (2018).

[2] E. Levi, R. Bojoi, F. Profumo, H.A. Toliyat, and S. Williamson, "Multiphase induction motor drives – a technology status review", *IET Electr. Power Appl.* 1(4), 489 (2007).

[3] F. Wilczyński, P. Strankowski, J. Guziński, M. Morawiec, and A. Lewicki, "Sensorless field oriented control for five-phase induction motors with third harmonic injection and fault insensitive feature", *Bull. Pol. Ac.: Tech.* 67(2), 253–262 (2019).

[4] H. Xu, H. A. Toliyat, and L. J. Petersen, "Rotor field oriented control of five-phase induction motor with the combined fundamental and third harmonic currents", in *Applied Power Electronics Conference and Exposition*, *2001. APEC 2001. Sixteenth Annual IEEE*, 2001, 1, pp. 392–398.

[5] P. Zhu, M. Qiao, Y. Wei, and Y. Xia, "Research on five-phase induction motor system control with third harmonic current injection", *The Journal of Engineering* (13), 2559–2563 (2017).

[6] A. Iqbal and E. Levi, "Space vector modulation schemes for a five-phase voltage source inverter", *European Conference on Power Electronics and Applications* 34(2), 119–140 (2006).

[7] N. Kim and W. Baik "A five-phase IM vector control system including 3rd current harmonics component", *IEEE 8th International Conference on Power Electronics and ECCE Asia 2011*, 2011, pp. 2519–2524.

[8] A. Lewicki, P. Strankowski, M. Morawiec, and J. Guziński, "Optimized Space Vector Modulation strategy for five phase voltage source inverter with third harmonic injection", in *Power Electronics and Applications* (*EPE'17 ECCE Europe*), *2017 19th European Conference on*, 2017.

[9] Z. Krzeminski, "Sensorless Control of Polyphase Induction Machines", *In Advanced Control of Electrical Drives and Power Electronic Converters*, pp. 3–26, ed. J. Kabziński, Springer International Publishing: New York, USA, 2017.

[10] J. Guzinski, H. Abu-Rub, and P. Strankowski, "*Variable Speed AC Drives with Inverter Output Filters*", Wiley, Hoboken, New Jersey, USA, 2015.

[11] T.G. Habetler, R. Naik, and T.A. Nondahl, "Design and implementation of an inverter output LC filter used for dv/dt reduction", *IEEE Transactions on Power Electronics* 17(3), 327–331 (2002).

[12] H. Akagi, H. Hasegawa, and T. Doumoto, "Design and performance of a passive EMI filter for use with a voltage–source PWM inverter having sinusoidal output voltage and zero common–mode voltage", *IEEE Transactions on Power Electronics* 19(4), 1069–1076 (2004).

[13] R. Seliga, W. Koczara, "Multiloop feedback control strategy in sine–wave voltage inverter for an adjustable speed cage induction motor drive system", *European Conference on Power Electronics and Applications EPE'2001*, Graz, Austria, 2001.

[14] J. Salomäki, M. Hinkkanen, and J. Luomi, "Sensorless Control of Induction Motor Drives Equipped With Inverter Output Filter", *IEEE Trans. on Industrial Electronics* 53(4), 1188–1197 (2006).

[15] M. Morawiec, P. Strankowski, A. Lewicki, and J. Guzinski, "Sensorless control of five-phase induction machine supplied by the VSI with output filter", *10th International Conference on Compatibility*, *Power Electronics and Power Engineering* (*CPE-POWERENG 2016*), Bydgoszcz, Poland, 2016.

[16] J. Guzinski, M. Morawiec, P. Strankowski, Z. Krzemiński, A. Lewicki, G. Kostro, and K. Woronowski, "Sensorless Multiscalar Control of Five-Phase Induction Machine with Inverter Output Filter", *The 19th Conference on Power Electronics and Applications* (*and Exhibition*), *EPE'17 ECCE* (*Energy Conversion Congress and Expo*) *Europe*, Warsaw, Poland, 2017.

[17] P. Strankowski, J. Guziński, F. Wilczyński, M. Morawiec, and A. Lewicki, "Open-Phase Fault Detection Method for Sensorless Five-Phase Induction Motor Drives with an Inverter Output Filter", *Power Electronics and Drives* 4(39), 189–200 (2019).

[18] Z. Krzeminski, "Nonlinear control of induction motor", *Proceedings of the 10th IFAC World Congress*, Munich, 1987.

[19] A. Isidori, "Nonlinear Control Systems", *Springer*, Berlin, 1995.

[20] M. Adamowicz, J. Guzinski, and Z. Krzeminski, "Nonlinear control of five phase induction motor with synchronized third harmonic flux injection", in *Smart Grid and Renewable Energy* (*SGRE*), *2015 First Workshop on*, 2015, pp. 1–6.

[21] H. Xu, H.A. Toliyat, and L.J. Petersen, "Rotor field oriented control of five-phase induction motor with the combined fundamental and third harmonic currents", *Sixteenth Annual IEEE Applied Power Electronics Conference and Exposition APEC 2001*, Anaheim, USA, 2001, 1, pp. 392–398.

[22] Huangsheng Xu, H.A. Toliyat, and L.J. Petersen, "Five-phase induction motor drives with DSPbased control system", *IEEE Trans. on Power Electronics* 17(4), 524–533 (2002).

[23] H. Abu-Rub, A. Iqbal, and J. Guzinski, "*High Performance Control of AC Drives with MATLAB/Simulink Models*", Wiley, Hoboken, New Jersey, USA.

[24] J. Salomäki, "Sensorless Control of AC Drives Equipped With An Inverter Output Filter", *Doctoral Dissertation*, Helsinki University of Technology, 2007.

[25] Z. Krzeminski, "Observer of induction motor speed based on exact disturbance model", in *Power Electronics and Motion Control Conference*, *2008. EPE-PEMC 2008. 13th*, Poznan, Poland, 2008, pp. 2294–2299.

[26] H. Guzman, J.A. Riveros, M.J. Duran, and F. Barrero, "Modeling of a five-phase induction motor drive with a faulty phase", in *15th International Power Electronics and Motion Control Conference* (*EPE/PEMC*), Novi Sad, Serbia, 2012.

[27] M.I. Masoud, S.M. Dabour, A.E.-W. Hassan, and E.M. Rashad, "Control of five-phase induction motor under open-circuit phase fault fed by fault tolerant VSI", in *IEEE 10th International Symposium on Diagnostics for Electrical Machines*, *Power Electronics and Drives* (*SDEMPED*), Guarda, Portugal, 2015, pp. 327–332.

[28] M. Bermudez, I. Gonzalez-Prieto, F. Barrero, H. Guzman, M.J. Duran, and X. Kestelyn, "Open-Phase Fault-Tolerant Direct Torque Control Technique for Five-Phase Induction Motor Drives", *IEEE Trans. on Industrial Electronics* 64(2), 902–911 (2017).

[29] Z. Peng, Z. Zheng, Y. Li, and Z. Liu, "Sensorless fault-tolerant control of multiphase induction machine using virtual winding and adaptive observer", in *IEEE Transportation Electrification Conference and Expo*, *Asia-Pacific* (*ITEC Asia-Pacific*), Harbin, China, 2017.

[30] A. Gonzalez-Prieto, I. Gonzalez-Prieto, M. Duran, and F. Barrero, "Efficient Model Predictive Control with Natural Fault-Tolerance in Asymmetrical Six-Phase Induction Machines", *Energies* 12(20), 3989 (2019).